2014 IEEE International Conference on Fuzzy Systems (FUZZ-IEEE)
July 6-11, 2014, Beijing, China

Fuzzy Classification of Orchard Pest Posture Based on Zernike Moments

Wen-Yong Li
Shang-Feng Du
Dept. Information and Electrical Engineering
China Agricultural University
Beijing, China
liwy@nercita.org.cn
13520760485@126.com

Ming Li
Mei-Xiang Chen
Chuan-Heng Sun
National Engineering Research Center for Information Technology in Agriculture
Beijing, China
lim@nercita.org.cn
chenmx@nercita.org.cn
sunch@nercita.org.cn

***Abstract*—Identification and count of orchard pests is very important in monitoring orchard pest population. The pests trapped by high-voltage grid show different postures and incomplete bodies, which increase the difficulty of image automated identification. Currently, most researches of pest image identification focus on feature extraction based on standard posture samples, without considering the influence from multi-pose of pests in natural scene. Consequently, the identification rates of these methods are low in practical orchard application. Using *Dichocrocis punctiferalis* (Guenee) as research object, this paper is directed towards a posture classification method for the orchard target pest identification. It aims at intensifying the performance of multi-pose pest identification system by utilizing Zernike moments as descriptors of shape characteristics. The input image is cropped automatically and further subjected to a number of preprocessing stages. The outcome of preprocessing stage is one processed image containing scaled and translated target pest. Then, the template number is determined according to the posture of target pest and the corresponding template parameters are obtained from the cluster centers by fuzzy C-mean clustering method. Experiment results show that the proposed shape feature is robust to changes caused by pest image shape rotation, translation, and/or scaling. And the highest accuracy of posture classification is 92.3% for orchard target pest *Dichocrocis punctiferalis* (Guenee) with multiple postures. It outperforms the method in reference [2] where the highest accuracy is 86.6%.**

Keywords—multi-pose; orchard pest identification; Zernike moments; image processing; fuzzy clustering

I. INTRODUCTION

Traditionally, pest management in orchards mainly relied on a regular spray program which was based on a schedule. Minimal use in pesticides is desired in pest control to cope with various problems caused by over-use of pesticides: acute toxicity to humans and animals, pest resistance to pesticides, change in pest status in agro-ecosystems, residue problems in environment[1].

With the increasing concern of environment impacts as well as pest control costs, integrated pest management (IPM) has now become one of the most effective and accurate ways to pest management in the orchard by discarding the regular spray program and relying more on actual presence, or likelihood of presence, of insects in the field[2]. Conventionally, identification and counting of insect specimens on the traps have been mostly relied on visual judgment by humans, and apply the most suitable pest management strategies according to the pest situation in an orchard estimated by specific insect distribution and population observed.

Automatic detecting system can be a significant contribution to objective estimation of a large number of pest insects in a short time period. The data obtained by visual judgment for pest densities were less accurate because of limited pest scouting expertise and the different levels of identification skills. Besides, potential critical control timing could be missed because of fatigues in continuous manually sampling and it requires long time for counting a large number of insects which can be alleviated with automation. There are some contributions on image-based automated insect identification research, but most of them focus on good image quality situations, like standard pest template with good pose, good wings show and consistent position of the insect in the image. Under good image quality situations, insect identification systems can obtain good results relatively using global features which represent general description for an insect image[3, 4]. Zhao et al.[5-7] evaluates the feasibility and reliability of assigning insects to three levels (order, superfamily and family) according to math-morphological features (MMF) and describes kinship among the insects of various categories within the same taxonomic level from the perspective of mathematical morphology. The ranked reliability of MMF for assigning insects to levels has been obtained using good insect specimens. The limitations of these systems are the sensitivity to noise and background clutter, strict requirement for insect pose, and a relatively complicated operation to

This research was supported by the Natural Science Foundation for the Youth (Grant No. 31301238) and the Beijing Natural Science Foundation (Grant No. 4132027).

acquire the image, thus, the insect samples studied in these research works are not representative of actual field-based images. Also, the global features result in poorer classification performance because these features are very sensitive to rotation, scale, translation, and viewpoint change, they can only handle insect images with very consistent and good poses. Our proposed features, Zernike moments(ZMs), have been utilized for extracting the shape and margin properties of orchard pests and describing the different and inconsistent pose of actual field-based orchard pests.

Since Zernike polynomials are orthogonal to each other, Zernike moments can represent the properties of an image with no redundancy or overlap of information between the moments. Besides, the Zernike moment descriptor has such properties as rotation invariance, robustness to noise and multi-level representation for describing the various shapes of pattern. Due to this characteristic, the magnitude of ZMs has been used widely in different types of applications [8-11].

In this paper, as the magnitude of ZMs is not scale and translation invariant[12, 13], we take pheromone-trapped target pest *Dichocrocis punctiferalis* (Guenee) as research object and propose a normalization method using the geometrical moments to produce scale and translation invariance. Then the template number is determined according to the posture of target pest and the template parameters are obtained from the cluster centers by fuzzy C-mean clustering method. Lastly, the field sample images of eight postures are tested using fuzzy classification method.

The organization of this paper is as follows. Section II introduces the Zernike moments (ZMs) transformation and their properties. The proposed approach has been discussed in detail in Section III. Section IV reports the experiments and results. The conclusion is given in the last section.

II. FUNDAMENTALS OF ZERNIKE MOMENTS

Basically, the Zernike moments are the extension of the geometric moments by replacing the conventional transform kernel $x^m y^n$ with orthogonal Zernike polynomials[9]. Since Zernike polynomials are orthogonal to each other, Zernike moments can represent the properties of an image with no redundancy or overlap of information between the moments [10]. Teh and Chin[14] show that among many moment-based shape descriptors, Zernike moment magnitude components are rotationally invariant and most suitable for shape description.

The Zernike basis function with n order and m m repetition is defined over a unit circle in the polar coordinates as follows:

$$V_{nm}(r,\theta) = R_{nm}(r) e^{jm\theta}, r \le 1 \tag{1}$$

Where { $R_{nm}(r)$ } is the real-valued 1-D radial polynomial which is defined as [12]

$$R_{nm}(r) = \sum_{s=0}^{\frac{n-|m|}{2}} c(n,m,s) r^{n-2s} \tag{2}$$

Where

$$c(n,m,s) = (-1)^s \frac{(n-s)!}{s!(\frac{n+|m|}{2}-s)!(\frac{n-|m|}{2}-s)!}.$$

In (2), n is a non-negative integer (n =0,1, $\cdots$, ∞) and m is an integer satisfying the conditions: $n-|m|$ is even and $|m| \le n$.

Zernike basis functions are orthogonal and satisfy

$$\int_0^{2\pi}\int_0^1 V_{nm}^*(r,\theta) V_{pq}(r,\theta) r dr d = \frac{\pi}{n+1}\delta_{np}\delta_{mq} \tag{3}$$

Where the symbol * denotes the complex conjugate and δ_{ab} satisfies

$$\delta_{ab} = \begin{cases} 1, & a=b \\ 0, & otherwise. \end{cases} \tag{4}$$

The 2-D ZMs for a continuous image function $f(r,\theta)$ are represented by

$$Z_{nm} = \frac{n+1}{\pi}\int_0^{2\pi}\int_0^1 f(r,\theta) V_{nm}^*(r,\theta) r dr d\theta \tag{5}$$

As can be seen from the definition, the Zernike moments can be seen as an inner product between the image function $f(r,\theta)$ and the Zernike basis function $\{V_{nm}(r,\theta)\}$.

For a digital image function, the 2-D ZMs are given as

$$Z_{nm} = \frac{n+1}{\pi}\sum_{(r,\theta)\in unitcircle}\sum f(r,\theta) V_{nm}^*(r,\theta) \tag{6}$$

When computing Zernike moments of an image, the centroid of the image is used to be origin and the coordinates of the image must be normalized into [0, 1] by a mapping transform. It must be mentioned that the Zernike moments is complex moments and the magnitude remains unchanged with the image rotation. Therefore, many applications use ZM magnitude as rotation invariant image features to describe the object's shape. In details, low-order moment feature vectors describe the whole view of target shape and high-order moment feature vectors represent the details of the target image[15].

III. METHODOLOGY

Fig. 1 represents the flowchart of the proposed approach. In this research, each image is a square-shaped region with the same number of rows and columns ($N \times N$).

There are visible tentacles in some pest images, however, some tentacles in other images are not visible. Besides, the pest tentacles are messy, which influences the pose and shape identification greatly. So the input images have been processed morphologically to eliminate the insect tentacles. There will be a binary image that represents the pest shape after image binarization and holes filling.

Then, as illustrated in Fig.1, the zeroth-order geometric moment and centroid are calculated. The scale value is obtained by combining the zeroth-order geometric moment with one predetermined value. Hereafter, the procedure is subjected to a normalized stage prior to calculation of the Zernike moments. This stage includes translation and scale to resolve the problem of dependency of Zernike moments on translation and scale. The translation stage translates the centroid of the pest object into the center of the image. Furthermore, the pest object is scaled using the scale value (a) which is calculated combining the zeroth-order geometric moment with one predetermined value.

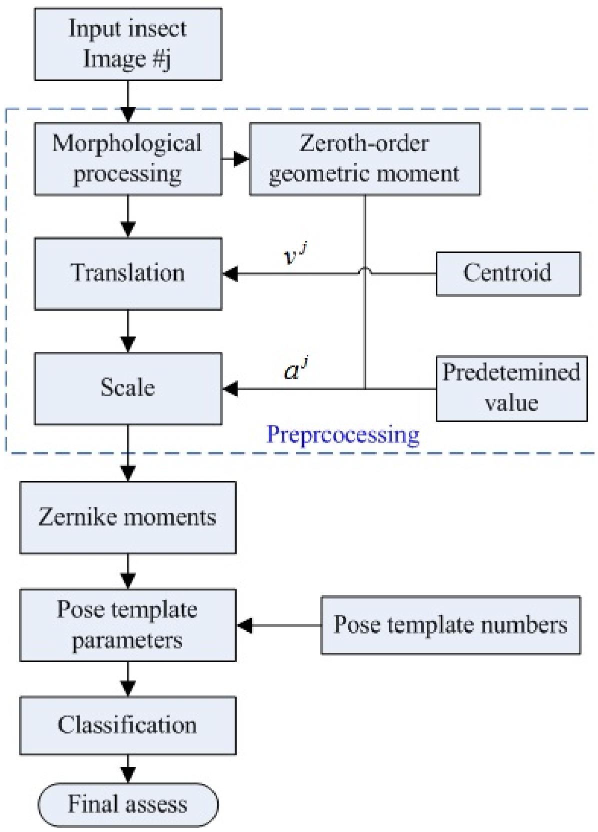

Fig.1. The flowchart of proposed approach

Now the input image is preprocessed and ready to be applied to the feature extraction section. Fig. 1 illustrates the feature extraction. Then template parameter vectors have been established for each posture which is determined by pest experts in actual field. Finally, the features are applied to a fuzzy classification method which is tested with different groups of input target pest images. In the rest of paper, each stage is discussed in detail.

A. *Preprocessing*

The operation in the preprocessing stage is divided into three steps. The first step is morphological process which includes conversion from RGB image to gray image, image binarization and elimination of pest tentacles using closing and opening morphological operations sequentially. Fig.2 illustrates two pest postures in different steps of the preprocessing stage.

Zernike moments are dependent on the translation and scaling of pest in images. In other words, the Zernike moments of two similar postures that are not equally scaled and translated are different. Thus, this suffering had better be compensated by normalizing the image using the Cartesian moments prior to calculation of the Zernike moments.

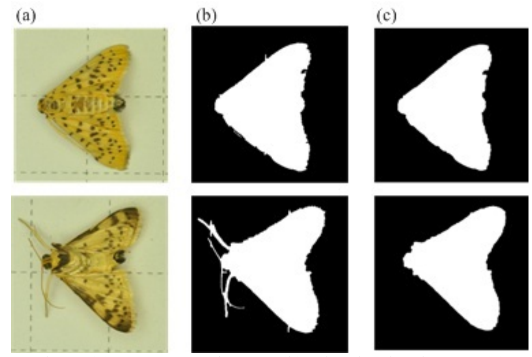

Fig.2. (a) Input RGB image, (b) Binarization image, (c) tentacles elimination image

Two steps have been employed to resolve the dependency problems. Firstly, Translation invariance is achieved by moving the centroid of each pest object to the centre of the corresponding image by using the centralized moments. The centroid of pest object has been calculated by the following equations[16, 17]:

$$\bar{x} = \frac{\sum_{i=0}^{N-1} \sum_{j=0}^{N-1} x f(x,y)}{\sum_{i=0}^{N-1} \sum_{j=0}^{N-1} f(x,y)} \tag{7}$$

$$\bar{y} = \frac{\sum_{i=0}^{N-1} \sum_{j=0}^{N-1} y f(x,y)}{\sum_{i=0}^{N-1} \sum_{j=0}^{N-1} f(x,y)} \tag{8}$$

Where $\bar{x}$ and $\bar{y}$ denote the column number and row number of the centroid, respectively. The pair (x, y) denotes the coordination of the image while $f(x, y)$ is the image function. The size of image is $N \times N$.

Then, the translation vector is calculated and given as follows:

$$\vec{v^j} = (round(\frac{N}{2}) - \bar{x}) * \vec{x} + (round(\frac{N}{2}) - \bar{y}) * \vec{y} \tag{9}$$

Where v^j is the translation vector. $round(\frac{N}{2})$ denotes the center of input image. j is the index of input image. Note that the centroid of the pest object coincides with the center of the input image after the translation.

In the second step, scale invariance is produced by alter-
ing size of each pest object so that its area (or pixel count for a binary image) is $m00 = \beta$, where β is a predetermined value. Eventually, the following equation is used to calculate the scaling coefficient: $a^j = \sqrt{\beta / m00}$,

where a denotes the suitable scaling coefficient for jth input image and $m00$ is zeroth order geometric moment which is equal to the area of the pest object and it can be computed as follows:

$$m00 = \sum_{i=0}^{N-1} \sum_{j=0}^{N-1} f(x, y) \tag{10}$$

Now, each pest object can be scaled properly using the suitable value a^j.

B. Feature Extraction

The computation of Zernike moments from an input image includes three steps: computation of radial polynomials, computation of Zernike basis functions and computation of Zernike moments by projecting the image onto the Zernike basis functions[11, 12]. The definition of these functions has been detailed in section II.

As the calculation of Zernike moments is described above, the coordinates of the image must be normalized into [0,1] by a mapping transform. Fig.3 depicts a general case of the mapping transform. Note that in this case, the pixels located on the outside of the circle are not involved in the computation of the Zernike moments. Eventually, the discrete form of the Zernike moments for an image with the size $N \times N$ is expressed as follows[12]:

$$\begin{aligned} Z_{nm} &= \frac{n+1}{\lambda_N} \sum_{x=0}^{N-1} \sum_{y=0}^{N-1} f(x, y) V_{nm}^*(x, y) \\ &= \frac{n+1}{\lambda_N} \sum_{x=0}^{N-1} \sum_{y=0}^{N-1} f(x, y) R_{nm}(\rho_{xy}) \exp(-jm\theta_{xy}) \end{aligned} \tag{11}$$

, where $0 \le \rho_{xy} \le 1$ and λ_N is a normalization factor. In the discrete implementation of Zernike moments, the normalization factor must be the number of pixels located in the unit circle by the mapping transform, which corresponds to the area of a unit circle, π, in the continuous domain[10]. The transformed distance ρ_{xy}, and the phase θ_{xy}, at the pixel of (x, y) are given by the following equations. Note that x and y denote the column and row number of the input image, respectively

$$\begin{aligned} \rho_{xy} &= \frac{\sqrt{(2x-N+1)^2 + (2y-N+1)^2}}{N}, \\ \theta_{xy} &= \tan^{-1}\left(\frac{N-1-2y}{2x-N+1}\right). \end{aligned} \tag{12}$$

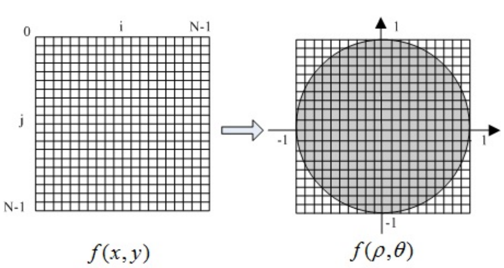

Fig.3. A general case of the mapping transform

Using (11) and (12), a final equation can be obtained which is only a function of x, y, m and n. We can simply calculate Zernike moments for every image without having difficulty with mapping functions using this equation.

It can be shown that rotating the object around the Z-axis do not influence the magnitude response of the Zernike moments[18, 19]. It can be uttered as follows:

$$Z_{nm}^r = Z_{nm} e^{-jm\alpha} \tag{13}$$

$$\left|Z_{nm}^r\right| = \left|Z_{nm} e^{-jm\alpha}\right| = \left|Z_{nm}\right| \tag{14}$$

Where Z_{nm}^r and Z_{nm} are the Zernike moments which are extracted from the rotated image and the original image, respectively. The rotation angle is α. The magnitude of the Zernike moment of original object and that of rotated object are equal. Thus, our proposed features are the magnitudes of Zernike moments which are proper descriptors of posture and shape characteristics. Fig. 4 illustrates the magnitude plots of some low order Zernike moments in the unit circle.

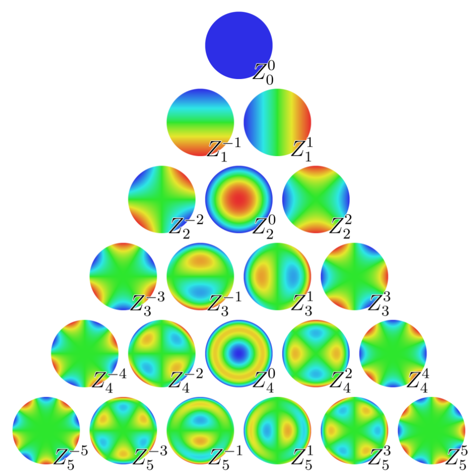

Fig.4. Plots of the magnitude of n ($n \le 5$) order Zernike basis functions in the unit circle.

C. Posture Templates Establishment

In order to realize the postures classification of target pest, posture templates and corresponding parameters should be established and computed. There are eight templates for each posture, and each template eigenvalue is equal to the clustering center which is obtained by fuzzy c-means clustering algorithms.

In the fuzzy c-means clustering algorithms, we can see that how the object partially or fully belongs to clusters depends on degree of membership of each object in different clusters. In other words, it represent the similarity a sample shares with each cluster according to a membership function whose values (called memberships) are between zero and one. Membership which is close to unity signifies a high degree of similarity between the sample and a cluster while membership being close to zero implies little similarity between the sample and that cluster.

Definition: $X = (x_1, x_2, \cdots, x_n)$ is a matrix which is constituted by p variables observations from n images and $V = \{v_1, v_2, \cdots, v_c\}$ is the cluster center of class

$c\ (2 \le c \le n)$,where

$v_i = (v_{i1}, v_{i2}, \cdots, v_{ip}), i = 1,2,\cdots,c.$

It is assumed that u_{ik} denotes the degree of membership that the kth sample X_k belongs to the ith cluster, where $0 \le u_{ik} \le 1, \sum_{i=1}^{c} u_{ik} = 1, c$ is total number of clusters. And the objective function of fuzzy c-means clustering is defined as[20]:

$$J(U,V) = \sum_{k=1}^{n}\sum_{i=1}^{c} u_{ik}^{m} d_{ik}^{2} \tag{15}$$

Where $U = (u_{ik})_{c\times n}$ is the matrix of degree of membership, and $d_{ik} = \|x_k - v_i\|$.

The final calculation of membership matrix U and cluster center V is the criterion of Fuzzy C-means clustering while they minimizes the objective function $J(U,V)$. Then, the result of cluster center V is used to be parameter eigenvalue of posture template.

D. Classification

Fuzzy rule-based systems have been applied mainly to control problems while more recently they have also been applied to pattern classification problems. For instance, they have been utilized in human skin color segmentation and classification[21], colony image classification[22], sequence processing and gesture recognition[23]. One advantage of a fuzzy rule-based system is its interpretability. The basic task of a classification technique is to divide n patterns, where n is a natural number, represented by vectors in a p-dimensional Euclidean space, into c , $2 \le c \le n$. The proposed fuzzy classification method is illustrated as followed.

Definition 1: the membership degree of one pest object belongs to posture c is denoted as:

$$\mu_{cn} = \frac{1}{1 + \left| Z_{nm} - Z_{nm}^{c} \right| / Z_{nm}^{c}} \tag{16}$$

where Z_{nm} is the n order Zernike moments of the pest posture which is needed to be classified, Z_{nm}^{c} is the corresponding n order Zernike moments of the template c ,

Definition 2: Weight coefficient vector of Zernike moment order is denotes as:

$$\alpha = [\alpha_2, \alpha_3, \cdots, \alpha_n]^T \ , \ \sum_{k=2}^{n} \alpha_k = 1 \tag{17}$$

Then the membership vector of this pest posture belonging to posture c is computed as followed:

$$\mu_c = \mu_{cn} \bullet \alpha = [\mu_1, \mu_2, \cdots, \mu_c] \tag{18}$$

The corresponding index of maximum component in vector μ_c is defined as the final cluster of this pest posture which is needed to be classified.

IV. Experiments and Results

A. Invariant properties of extracted pest posture features

To evaluate the invariant performance of the proposed image feature, eight binary shapes of *Dichocrocis punctiferalis* (Guenee) have been used in this experiment. Fig. 5 shows eight images and the size of each image is $N \times N$ (N =480). (a) is the original image. (b)~(d) are the images rotated by 45° , 90° and 180° angle, respectively. (e) and (f) are the images translated by 20 pixels to right and upside, respectively. (g) and (h) are the images scaled by 120% and 50% factor, respectively.

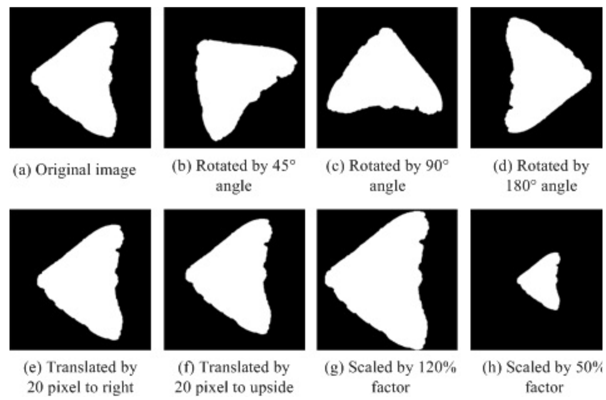

Fig.5. Rotation, translation and scaling insect image

The Zernike moments ($n \le 5$) are extracted, which are listed in Table I and II.

TABLE I
ZERNIKE MOMENTS FEATURE OF THE SAME INSECT WITH DIFFERENT GEOMETRIC SHAPE

	Z_{20}	Z_{22}	Z_{31}	Z_{33}	Z_{40}
(a)	0.4516	0.0199	0.0102	0.0225	0.4111
(b)	**0.4511**	0.0200	0.0083	0.0228	0.4104
(c)	0.4516	0.0199	0.0102	0.0225	0.4111
(d)	0.4516	0.0199	0.0102	0.0225	0.4111
(e)	0.4516	0.0199	0.0102	0.0225	0.4111
(f)	0.4516	0.0199	0.0102	0.0225	0.4111
(g)	**0.4523**	0.0200	0.0090	0.0227	0.4111
(h)	**0.4481**	0.0197	0.0100	0.0221	0.4107

TABLE II
TABLE I (CONT)

	Z_{42}	Z_{44}	Z_{51}	Z_{53}	Z_{55}
(a)	0.0661	0.0007	0.0380	0.0904	0.0046
(b)	0.0663	0.0009	0.0359	0.0915	0.0047
(c)	0.0662	0.0007	0.0380	0.0904	0.0046
(d)	0.0662	0.0007	0.0380	0.0904	0.0046
(e)	0.0661	0.0007	0.0380	0.0904	0.0046
(f)	0.0661	0.0007	0.0380	0.0904	0.0046
(g)	0.0663	0.0005	0.0367	0.0911	0.0046
(h)	0.0656	0.0006	0.0374	0.0891	0.0045

As we can see from table I and II, these extracted features are highly consistent for all images (a)~(h). It illustrates that the proposed geometric normalized algorithm has good performance in rotation invariance, translation invariance and scale invariance of orchard pest images. Meanwhile, we can discover that there are some subtle differences among them, which are caused by image pixels interpolation in the process of image rotation and scale. And it will bring slight difference between the edges of these transformed images and the original image.

B. Posture Templates and Parameters Calculation

There are many different postures of orchard pests which are trapped by sex pheromone lure. According to the experience of insect experts, eight postures are determined based on the facts that the upward body part (either notum or abdomen) and the stretched degree of wings. Fig.6 shows the images of eight postures. They are denotes as P1~P8. There are four postures for upward notum and abdomen, respectively, with different stretched degree of wings which are fully stretched wings, half stretched wings, contractive wings and one contractive wing, one stretched wing. So this paper sets up eight templates for this eight posture types.

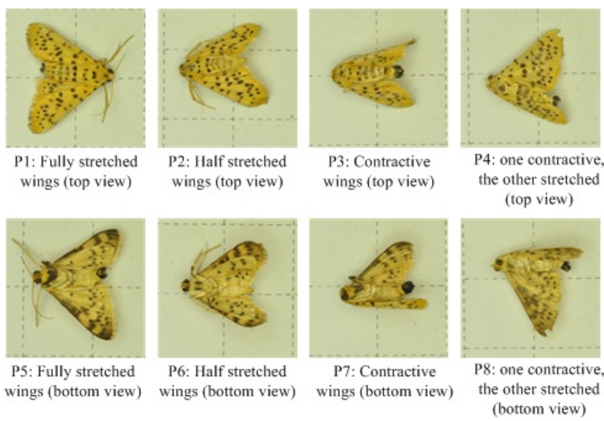

Fig.6. Eight common postures of *Dichocrocis punctiferalis* (Guenee) in actual field-based images

In single template identification, the eigenvalue matrix in training set is used to be the template parameters of corresponding posture using fuzzy c-means cluster technology. In the training set, 50 images for each template are selected by insect expert. The template eigenvalue based on Zernike moments $Z_{nm}(n=5, m \le n)$ are showed in Table III and IV.

TABLE III
TEMPLATE EIGENVALUES OF THE EIGHT POSTURES

	Z_{20}	Z_{22}	Z_{31}	Z_{33}	Z_{40}
P1	0.4424	0.0171	0.0120	0.0294	0.3835
P2	0.4449	0.0170	0.0117	0.0274	0.3901
P3	0.4549	0.0048	0.0061	0.0186	0.4142
P4	0.4554	0.0018	0.0064	0.0195	0.4150
P5	0.4492	0.0110	0.0079	0.0257	0.4048
P6	0.4493	0.0158	0.0072	0.0253	0.4037
P7	0.4517	0.0172	0.0024	0.0201	0.4138
P8	0.4521	0.0160	0.0039	0.0210	0.4135

TABLE IV
TABLE III (CONT)

	Z_{42}	Z_{44}	Z_{51}	Z_{53}	Z_{55}
P1	0.0555	0.0024	0.0465	0.1161	0.0040
P2	0.0567	0.0013	0.0418	0.1099	0.0038
P3	0.0185	0.0071	0.0223	0.0790	0.0016
P4	0.0077	0.0062	0.0271	0.0826	0.0011
P5	0.0379	0.0017	0.0276	0.1038	0.0020
P6	0.0534	0.0022	0.0294	0.1007	0.0029
P7	0.0586	0.0044	0.0088	0.0821	0.0062
P8	0.0542	0.0034	0.0070	0.0867	0.0051

C. Posture Classification

According to the classification by insect experts, the different posture images of *Dichocrocis punctiferalis* (Guenee) are captured, which are consist of 60, 60, 40, 40, 60, 60, 40, 40 images for P1~P8, respectively. The total number of images is 400 for posture classification test using the proposed method.The template number c is 8.

As we can see from table III and IV, Z_{20}, Z_{40}, Z_{44} and Z_{55} are so similar among all posture types that they are assigned low weight. On the contrary, the other eginvalues Z_{22}, Z_{31}, Z_{33}, Z_{42}, Z_{51} and Z_{53} are assigned high weight relatively. The weight coefficient vector of Zernike moment order is:

$$\alpha = \left[\frac{1}{20}, \frac{4}{30}, \frac{4}{30}, \frac{4}{30}, \frac{1}{20}, \frac{4}{30}, \frac{1}{20}, \frac{4}{30}, \frac{4}{30}, \frac{1}{20} \right]^T .$$

Using equation (16), (17) and (18), the results are calculated and showed in Table V.

TABLE V
CLASSIFICATION RESULTS

Posture type	Manually	PROPOSED METHODE	ERROR NUMBERS	ACCURACY
P1	60	53	7	88.3%
P2	60	55	5	91.7%
P3	40	36	4	90%
P4	40	33	7	82.5%
P5	60	54	6	90%
P6	60	53	7	88.3%
P7	40	37	3	92.5%
P8	40	34	6	85%

As we can see from table V, the classification results of the proposed method show good performance in postures identification and it is consistent with the results of expert's selection. The best classification posture is P7 and its accuracy is 92.5%.

In reference [2], the highest accuracy is 86.6% using the combination model. And the total number of extracted features is 154, 54 global features and 100 local features, respectively. However, there are only 10 Zernike moment values for each posture. So the calculation complexity of the proposed method is much low than that of reference [2]. Besides, we also found some significant and meaningful results:

(1) There are more cross misclassification between posture P1 and P5. In Fig.8, (a) and (c) are the images which are captured at notum upward and abdomen upward view of

one same *Dichocrocis punctiferalis* (Guenee), respectively. (b) and (d) are their corresponding binarization images. As we can see from Fig.7, the wings of this pest are stretched fully in this two cases. After morphological operations for tentacles elimination, the two posture shapes are similar in the same image collection environment, thus the value of Zernike moments are close to each other, so that there are cross misclassification phenomenon.

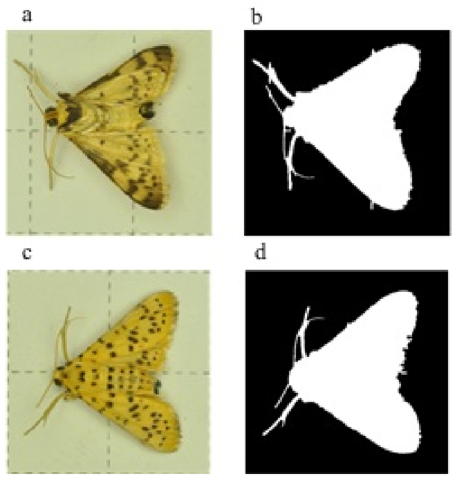

Fig.7. Two postures of *Dichocrocis punctiferalis* (Guenee) in actual field-based image

(2) It is difficult to determine the stretched degree of the wings between posture P2 and P3, P7 and P8. So there is some uncertainty when insect experts classify many similar postures. It is another reason to affect the classification accuracy.

(3) Another discovery is that there are some differences in shape between the RGB image and its corresponding binarization result because of incomplete body and inconsistent body color in some preprocessed images. As it is showed in Fig.8, (a) is one *Dichocrocis punctiferalis* (Guenee) image with posture P8, and we can found that there is one imperfect edge denoted with red ellipse in its binarization image (b). The shape in binarization image is much different with the original RGB image, so it is possible to misclassify the posture.

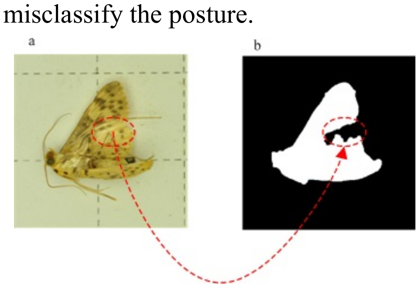

Fig.8. Difference between original image and binarization image of *Dichocrocis punctiferalis* (Guenee) of P8 posture

V. Conclusion

In this paper, a novel method was introduced for posture classification of orchard target pest *Dichocrocis punctiferalis* (Guenee) to achieve better identification performance under different postures. The Zernike moments are utilized as the descriptors of posture characteristics of pest. The input images are preprocessed containing morphological operations, elimination of insect tentacles and invariance transformation. The template number is determined according to the posture of target pests in actual field and the template parameters are obtained from the cluster centers using fuzzy C-mean clustering method before postures classification. The results showed that the highest accuracy of template matching is 92.5% for sex pheromone-trap pests with multiple postures. It can be concluded from the experimental results that the posture classification method has potential application for pest identification and counting.

Advanced analysis on posture similarity and imperfect edge are conducted in this research. Template numbers and more adaptive morphological preprocessed algorithm need to be further researched.

It must be mentioned that the utilized posture templates are different with the change of target pest species. The researchers are advised to determine his posture template numbers for his research object by experienced insect experts and then find the best template parameter vector.

References

[1] J. Cho, J. Choi, M. Qiao, and C.-w. Ji, "Automatic identification of whiteflies, aphids and thrips in greenhouse based on image analysis," Internatinal journal of mathematics and computers in simulation, vol. 1, pp. 46-57, 2007.

[2] C. Wen and D. Guyer, "Image-based orchard insect automated identification and classification method," Computers and Electronics in Agriculture, vol. 89, p. 110~115, 2012.

[3] T. Arbuckle, S. Schroder, V. Steinhage, and D. Wittmann, "Biodiversity informatics in action: Identification and monitoring of bee species using ABIS," Proceeding of the 15th International Symposium on Informatics for Environmenttal Protection, vol. Metropolis Press, pp. 425-430, 2001.

[4] S. M. A. Ashaghathra, P. Weckler, J. Solie, M. Stone, and A. Wayadande, "Identifying Pecan Weevils through Image Processing Techniques Based on Template Matching," ASAE Annual Meeting, 2007.

[5] Z. H. Qing, S. Z. Rui, and Y. X. Wen, "Use of math-morphological features in insect taxonomy.I. At the order level," Acta Entomologica Sinica, vol. 46, pp. 45-50, 2003.

[6] Z. H. Qing, S. Z. Rui, and Y. X. Wen, "Use of math-morphological features in insect taxonomy.II. At superfamily level," Acta Entomologica Sinica, vol. 46, pp. 201-208, 2003.

[7] Z. H. Qing, S. Z. Rui, and Y. X. Wen, "Use of math-morphological features in insect taxonomy.III. At the family level," Acta Entomologica Sinica, vol. 46, pp. 339-344, 2003.

[8] Z. Chen and S. K. Sun, "A Zernike Moment Phase-Based Descriptor for Local Image Representation and Matching," IEEE Transactions on Image Processing, vol. 19, pp. 205-219, 2010.

[9] S. Li, M. C. Lee, and C. M. Pun, "Complex Zernike Moments Features for Shape-Based Image Retrieval," IEEE Transactions on System, Man and Cybernetics, Part A: System and Humans, vol. 39, pp. 227-237, 2009.

[10] A. Tahmasbi, F. Saki, and S. B. Shokouhi, "Classification of benign and malignant masses based on Zernike moments," Comput Biol Med, vol. 41, pp. 726-35, Aug 2011.

[11] X. Li and A. Song, "A New Edge Detection Method Using Gaussian-Zernike Moment Operator," in: Proceedings of the IEEE, 2nd International Asia Conference on Informatics in Control, Automation and Robotics, pp. 276-279, 2010.

[12] S.-K. Hwang and W.-Y. Kim, "A novel approach to the fast computation of Zernike moments," Pattern Recognition, vol. 39, pp. 2065-2076, 2006.

[13] C. Singh, E. Walia, and R. Upneja, "Accurate calculation of Zernike moments," Information Sciences, vol. 233, pp. 255-275, 2013.

[14] C. H. Teh and R. T. Chin, "On Image Analysis by the Methods of Moments," IEEE Transactions on pattern analysis and machine itelligence, vol. 10, pp. 496-513, 1988.

[15] L. M. Fu, H. H. Jun, and H. Y. Xiang, "Application of PCA in dimension reduction of image Zernike moments feature," Journal of Computer Application, vol. 37, pp. 696-698, 2007.

[16] W. K. Pratt, Digital Image Processing: PIKS Inside, Third Edition vol. Chapter 18, 2002.

[17] Y. Y. Bin, G. J. Sheng, and R. X. Qin, "Fruit shape classification based on Zernike moments," Journal of Jiangsu University(Natural Science Edition), vol. 28, pp. 1-4, 2007.

[18] W. Y. Kim and Y. S. Kim, "A region-based shape descriptor using Zernike moments," Signal Processing: Image Communication, pp. 95-102, 2000.

[19] H. K. Kim and J. D. Kim, "Region-based shape descriptor invariant to rotation, scale and translation," Signal Processing: Image Communication, pp. 87-93, 2000.

[20] R. L. Cannon, J. V. Dave, and J. C. Bezdek, "Efficient implementation of the Fuzzy c-Means Clustering Algorithms," IEEE Transactions on pattern analysis and machine itelligence, vol. PAMI-8, pp. 248-256, 1986.

[21] C. F. Juang, S. H. Chiu, and S. J. Shiu, "Fuzzy system learned through fuzzy clustering and support vector machine for human skin color segmentation," IEEE Transactions on System, Man and Cybernetics, Part A: System and Humans, vol. 37, pp. 1077-1087, 2007.

[22] X. J. Ban, X. L. Lv, and J. Chen, "Colony image retrieval and classification using fuzzy similarity measure and fuzzy clustering method," Joint 48th IEEE conference on decision and control and 28th chinese control conference, vol. December 16-18, pp. 7777-7782, 2009.

[23] C. F. Juang and K. C. Kun, "A recurrent fuzzy network for fuzzy temporal sequence processing and gesture recognition," IEEE Transactions on System, Man and Cybernetics, Part B: cybernetics, vol. 35, pp. 646-658, 2005.